RESEARCH ARTICLE

Synthesis, Anti-Inflammatory and Anticancer Activity Evaluation of Some Novel Acridine Derivatives

Sudhir S. Hunge[1], Amol P. Patil[2], K. Thejomoorthy[3], Pallawi[4], Gigi G.P.[5], Naveen Kumar B.S.[6], Kayumov Ganisher Olimovich[7] and Vaibhav Gawade[8*]

[1]P.G. Department of Chemistry, Chintamani College of Science, Pombhurna, Dist. Chandrapur, Maharashtra - 442918; Gondwana University, Gadchiroli (M.S.).

[2]Department of Pharmacology, TVES Honorable Loksevak Madhukarrao Chaudhari College of Pharmacy, Faizpur 425503, Maharashtra, India.

[3]University College of Pharmaceutical Sciences, Acharya Nagarjuna University, NH16, Nagarjuna Nagar, Guntur, Andhra Pradesh 522510.

[4]Kashi Institute of pharmacy, Varanasi, Mirzamurad, Khalispur, Uttar Pradesh 221307.

[5]Department of Pharmaceutical Chemistry, College of Pharmacy, Shaqra University, Dawadimi, Saudi Arabia.

[6]Saveetha Institute of Medical and Technical Sciences, Chennai, Tamil Nadu, India.

[7]Department of Folk Medicine and Pharmacology, Fergana Medical Institute of Public Health, Yangi Turon 2A, Fergana - 150100, Uzbekistan.

[8]Oriental College of Pharmacy, Navi Mumbai, Maharashtra, India.

***Corresponding Author:**
Dr. Vaibhav Gawade,
Assistant Professor, Oriental College of Pharmacy, Navi Mumbai.
E-mail: gawadevaibhav6060@gmail.com

Abstract

Acridine and its derivatives have long occupied a special place in medicinal chemistry owing to their broad-spectrum pharmacological activities. In the present study, a series of twelve novel acridine-based compounds (ACD-1 through ACD-12) were designed, synthesized, and characterized with the primary objective of identifying potent anti-inflammatory and anticancer agents with an acceptable safety profile. The synthetic route involved a Doebner–Miller condensation reaction followed by nucleophilic substitution, yielding target molecules bearing diverse substituents at the 9-position and on the peripheral aromatic rings. All synthesized compounds were characterized by ^{1}H NMR, ^{13}C NMR, IR, and high-resolution mass spectrometry (HRMS). For anti-inflammatory screening, the compounds were evaluated through in vitro albumin denaturation inhibition, membrane stabilization, and heat-induced hemolysis assays. Compounds ACD-5, ACD-8, and ACD-11 emerged as the most promising anti-inflammatory agents, with ACD-8 showing 78.4% inhibition of albumin denaturation at 500 µg/mL, outperforming the standard drug diclofenac sodium (72.1%). The anticancer potential of the synthesized compounds was assessed against four human cancer cell lines — MCF-7 (breast), HeLa (cervical), A549 (lung), and HCT116 (colon) — using the MTT assay. ACD-5 and ACD-11 exhibited remarkable cytotoxicity, with IC_{50} values of 3.24 µM and 4.11 µM against MCF-7 cells, respectively, surpassing the reference drug doxorubicin (IC_{50} = 5.82 µM) in selectivity. Molecular docking studies revealed that these compounds interact favorably with COX-2 and topoisomerase II enzymes through hydrogen bonding and π–π stacking interactions. Furthermore, in silico ADMET profiling indicated drug-like properties consistent with Lipinski's Rule of Five for most derivatives. The combined biological data from this study strongly suggest that these novel acridine derivatives warrant further investigation as leads in anti-inflammatory and anticancer drug discovery.

Keywords: Acridine derivatives; Anti-inflammatory; Anticancer; MTT assay; Molecular docking; Albumin denaturation; COX-2 inhibition; Topoisomerase II; ADMET; Drug discovery.

How To Cite This Article: Hunge SS, Patil AP, Thejomoorthy K, Pallawi, Gigi GP, Kumar Naveen BS, Olimovich KG, Gawade V. Synthesis, Anti-Inflammatory and Anticancer Activity Evaluation of Some Novel Acridine Derivatives. Int J Drug Deliv Technol. 2026;16(10s): 533-543; DOI: 10.25258/ijddt.16.10s.66

1. INTRODUCTION

Inflammation and cancer are two of the most extensively investigated disease conditions in contemporary biomedical research, not merely because of their alarming global prevalence but also due to the deeply intertwined molecular mechanisms that connect them. Chronic, unresolved inflammation has now been recognized as a significant risk factor in the initiation and progression of several malignancies, and this knowledge has fundamentally reshaped how researchers approach the development of new therapeutic molecules.[1] The discovery that prostaglandin biosynthesis, mediated primarily through the cyclooxygenase-2 (COX-2) enzyme, drives both inflammatory cascades and tumor-promoting microenvironments has given rise to a new generation of dual-activity anti-inflammatory/anticancer drug candidates.[2]

Acridine, a tricyclic planar aromatic compound composed of two benzene rings fused on either side of a central pyridine ring, has been part of the pharmacological arsenal for over a century. Its first therapeutic use dates back to the early twentieth century when acriflavine, an aminoacridine derivative, was employed as an antiseptic. Since then, acridine scaffolds have found roles in a surprisingly diverse range of biological activities, including antiprotozoal, antibacterial, antiviral, antifungal, and more recently, pronounced anticancer and anti-inflammatory activities.[3] The planar aromatic system of acridine permits intercalation into DNA base pairs, an interaction mode that underlies the cytotoxic effects of several acridine-based drugs. Perhaps the most notable clinical example is amsacrine (m-AMSA), an acridine-based topoisomerase II inhibitor used in the treatment of acute leukemia and lymphoma.[4]

Despite the well-established therapeutic potential of acridine derivatives, challenges remain in optimizing the balance between potency and selectivity. Many earlier-generation acridines exhibited significant cardiotoxicity and non-selective DNA binding, limiting their clinical application.[5] Modern synthetic approaches, however, have enabled the strategic decoration of the acridine scaffold with carefully chosen substituents that not only enhance target affinity but also modulate physicochemical properties relevant to bioavailability and reduced toxicity. Introducing electron-donating or electron-withdrawing groups at specific positions of the acridine ring, or appending pharmacophoric moieties such as sulfonamide, hydrazide, or Schiff base fragments, has been shown to considerably amplify the biological response.[6]

In terms of anti-inflammatory pharmacology, acridine derivatives have been shown to inhibit nuclear factor-κB (NF-κB) signaling, suppress the production of pro-inflammatory cytokines such as TNF-α, IL-1β, and IL-6, and block the enzymatic activity of COX-2 and 5-lipoxygenase (5-LOX). Several recent studies have highlighted 9-aminoacridine and 9-chloroacridine scaffolds as privileged structures in developing COX-2 inhibitors with minimal gastrointestinal side effects.[7] In the anticancer domain, acridine derivatives interact with topoisomerase I and II enzymes, disrupt spindle assembly, and induce mitochondrial-mediated apoptosis, making them relevant to multiple therapeutic targets across cancer types.[8]

The present work was thus motivated by the need to develop novel acridine-based hybrid molecules capable of addressing both inflammatory and neoplastic conditions through rational design. By incorporating electron-donating methoxy groups, fluorine atoms, and heterocyclic extensions into the 9-position of the acridine nucleus, we aimed to create compounds that could simultaneously interact with COX-2's hydrophobic binding pocket and the DNA-intercalation domain of topoisomerase II. The novelty of the current work lies in the structural design of these hybrid derivatives, the comprehensiveness of in vitro biological evaluation, and the integration of in silico molecular docking to rationalize the observed structure-activity relationships. This paper presents the synthesis, spectral characterization, biological screening, and computational analysis of twelve new acridine derivatives with the hope that these findings will provide meaningful contributions to the ongoing effort of discovering effective and safer anti-inflammatory and anticancer drug candidates.[9]

2. MATERIALS

All chemicals and solvents utilized throughout this study were of analytical reagent grade unless otherwise specified, and no further purification was performed prior to use when their purity was confirmed. The primary starting material, acridine (purity ≥ 98%), was procured from Sigma-Aldrich (St. Louis, MO, USA). Anthranilic acid, various substituted benzaldehydes (4-methoxybenzaldehyde, 4-fluorobenzaldehyde, 3-nitrobenzaldehyde, 4-chlorobenzaldehyde, 2-hydroxybenzaldehyde, 4-dimethylaminobenzaldehyde, 3,4-dichlorobenzaldehyde, 4-trifluoromethylbenzaldehyde), phosphorus oxychloride

($POCl_3$), hydrazine hydrate (80%), glacial acetic acid, and polyphosphoric acid were all purchased from Sigma-Aldrich or TCI Chemicals (Tokyo, Japan) and used as received.

Organic solvents including ethanol (absolute, 99.5%), methanol (HPLC grade), dimethyl sulfoxide (DMSO, ≥99.9%), chloroform, ethyl acetate, n-hexane, dichloromethane, and diethyl ether were supplied by Merck KGaA (Darmstadt, Germany). Thin layer chromatography (TLC) was performed on pre-coated silica gel 60 F_{254} aluminum sheets (Merck), and visualization was achieved using UV light (254 and 365 nm) and iodine vapor. Column chromatography was carried out on silica gel (100–200 mesh, SRL Chemicals, India) as the stationary phase, with gradient solvent systems of n-hexane/ethyl acetate as the mobile phase.

For spectral characterization, ^1H and ^{13}C NMR spectra were recorded on a Bruker AVANCE III 400 MHz spectrometer (Bruker BioSpin, Rheinstetten, Germany) using DMSO-d_6 as the solvent, with tetramethylsilane (TMS) as the internal reference. Chemical shifts are reported in parts per million (δ, ppm), and coupling constants (J) are given in hertz (Hz). Infrared (IR) spectra were obtained on a PerkinElmer Spectrum Two FT-IR spectrometer in the range of 4000–400 cm^{-1} using KBr pellets. High-resolution mass spectrometry (HRMS) was performed on a Waters Q-TOF Synapt G2 mass spectrometer using electrospray ionization (ESI) in positive mode. Melting points of all synthesized compounds were determined using a Stuart SMP10 melting point apparatus (Bibby Scientific, UK) and are uncorrected.

For biological evaluations, bovine serum albumin (BSA, Fraction V, ≥96%), human red blood cells (freshly obtained from healthy volunteers under institutional ethical approval), phosphate-buffered saline (PBS, pH 7.4), diclofenac sodium (reference anti-inflammatory standard), doxorubicin (anticancer positive control), and the MTT reagent (3-(4,5-dimethylthiazol-2-yl)-2,5-diphenyltetrazolium bromide) were sourced from Sigma-Aldrich. All cell culture media (DMEM, RPMI-1640), fetal bovine serum (FBS), antibiotics (penicillin-streptomycin), and trypsin-EDTA solution were acquired from Gibco (Thermo Fisher Scientific, Waltham, MA, USA). Cancer cell lines MCF-7, HeLa, A549, and HCT116 were obtained from the National Centre for Cell Science (NCCS), Pune, India, and maintained under standard conditions (37°C, $5CO_2$, humidified atmosphere).

3. METHODS

3.1. General Synthesis of 9-Substituted Acridine Derivatives

The synthesis of novel acridine derivatives was accomplished using a two-step sequential approach inspired by the classical Bernthsen and Doebner–Miller condensation reactions, adapted with modifications to improve yield and purity. In the first step, 2-aminobenzophenone (or appropriately substituted anthranilic acid) was condensed with substituted aldehydes in the presence of zinc chloride ($ZnCl_2$) as a Lewis acid catalyst in diphenyl ether at 200°C for 4–6 hours, yielding the corresponding 9-substituted acridine intermediates. In the second step, selective chlorination at the 9-position was achieved using $POCl_3$ to activate the carbonyl for subsequent nucleophilic displacement. The 9-chloroacridine intermediates were then reacted with various amine nucleophiles or heterocyclic moieties in the presence of triethylamine as a base in refluxing ethanol to afford the final target compounds ACD-1 through ACD-12. Reactions were monitored by TLC at regular intervals. Following reaction completion, the crude products were subjected to column chromatography to yield pure compounds, which were then recrystallized from ethanol/water (8:2, v/v) to obtain analytically pure samples. Yields ranged from 48% to 79%.[10]

3.2. Formulation Design of Selected Acridine Derivatives

Based on preliminary solubility screening, the most biologically active compounds (ACD-5, ACD-8, and ACD-11) were selected for formulation development. Eight formulations (F1–F8) were designed to optimize the solubility, dissolution profile, and potential oral bioavailability of these compounds. Solid dispersion techniques, nanosuspension preparation, and lipid-based drug delivery systems were explored. Excipients such as PVP K30, HPMC E15, Poloxamer 188, Cremophor EL, Soluplus, and Kollicoat IR were selected based on compatibility studies and their established roles in enhancing the aqueous dissolution of BCS Class II drugs. The formulation compositions are summarized in Table 1.

Table 1: Formulation design of acridine derivative-based preparations (F1–F8)

Formulation	Drug	Drug Conc.	Delivery System	Primary Excipient	Secondary Excipient	Solubilizer	Ratio (D:E)	Preparation Method
F1	ACD-5	10 mg	Solid Dispersion	PVP K30	SLS	PEG 400	1:5	Hot-Melt Extrusion
F2	ACD-5	10 mg	Nanosuspension	Poloxamer 188	HPMC E15	Tween 80	1:3	Probe Sonication
F3	ACD-8	15 mg	Self-Emulsify. (SEDDS)	Cremophor EL	Capmul PG-8	Transcutol P	1:9	Vortex mixing
F4	ACD-8	15 mg	Solid Dispersion	Soluplus	Kollicoat IR	PVP K17	1:7	Spray Drying
F5	ACD-11	20 mg	Nanoparticle (PLGA)	PLGA (50:50)	PVA	Span 80	1:4	Nanoprecipitation
F6	ACD-11	20 mg	Cyclodextrin Complex	β-Cyclodextrin	HPMC E5	PEG 6000	1:2	Kneading Method
F7	ACD-5	10 mg	Liposomal Formulation	DPPC	Cholesterol	DSPE-PEG	1:6	Thin Film Hydration
F8	ACD-8	15 mg	Microemulsion	IPM (oil phase)	Tween 80	PEG 400	1:8	Titration Method

Abbreviations: SLS = Sodium Lauryl Sulfate; PEG = Polyethylene Glycol; HPMC = Hydroxypropyl Methylcellulose; SEDDS = Self-Emulsifying Drug Delivery System; PLGA = Poly(lactic-co-glycolic acid); PVA = Polyvinyl Alcohol; DPPC = Dipalmitoylphosphatidylcholine; DSPE = Distearoylphosphoethanolamine; IPM = Isopropyl Myristate; D:E = Drug to Excipient ratio.

3.3. *In Vitro* Anti-Inflammatory Activity

3.3.1. Albumin Denaturation Inhibition Assay

The protein denaturation inhibition method was employed as a well-validated in vitro model for assessing anti-inflammatory activity, based on the established pathophysiological principle that denaturation of proteins during inflammatory processes contributes to tissue injury. The assay was performed according to the modified protocol of Sakat et al. with minor adaptations. Briefly, a 0.5% (w/v) solution of bovine serum albumin (BSA) in PBS (pH 6.4) was prepared fresh on the day of the experiment. Test compounds were dissolved in DMSO and diluted serially in PBS to achieve concentrations of 100, 200, 300, 400, and 500 µg/mL (DMSO concentration kept below 1% v/v). To 1.0 mL of BSA solution, 0.05 mL of the test compound solution was added, and the pH was adjusted to 6.4 using 1 N HCl. The reaction mixtures were incubated at 37°C for 20 minutes and subsequently subjected to thermal denaturation at 72°C for 5 minutes in a precisely temperature-controlled water bath. After cooling to room temperature, the absorbance of each turbid suspension was measured at 660 nm using a UV-Vis spectrophotometer (Shimadzu UV-1800, Japan). Diclofenac sodium at corresponding concentrations served as the positive control. Blank solutions devoid of test compound were prepared identically. The percentage inhibition of denaturation was calculated using the formula: % Inhibition = $[(Abs_{control} - Abs_{sample}) / Abs_{control}] \times 100$. All determinations were performed in triplicate, and IC_{50} values were determined by non-linear regression analysis.[11]

3.3.2. Heat-Induced Hemolysis Inhibition Assay

The membrane-stabilizing activity of synthesized compounds was assessed through the heat-induced hemolysis assay using freshly prepared human erythrocytes. Whole blood was collected from healthy non-medicated volunteers (with informed consent under institutional ethics approval No. PHARM/IEC/2024/018) into EDTA-containing vacutainers and was washed three times with isotonic PBS (pH 7.4) by centrifugation at 3000 rpm for 10 minutes. A 10% (v/v) erythrocyte suspension was prepared in isotonic PBS. Equal volumes (1 mL) of the erythrocyte suspension and test compound solutions at varying concentrations (100–500 µg/mL) were mixed in

sealed centrifuge tubes. The mixtures were placed in a water bath at 56°C for 30 minutes. Control tubes containing erythrocytes without drug and vehicle-only controls were run simultaneously. After heat treatment, the tubes were cooled on ice and centrifuged at 2500 rpm for 10 minutes. The hemoglobin released into the supernatant was measured spectrophotometrically at 540 nm. Diclofenac sodium was used as the reference standard, and the percentage protection against hemolysis was calculated as:

$\%\ \text{Protection} = [(\text{Abs}_{\text{control}} - \text{Abs}_{\text{sample}}) / \text{Abs}_{\text{control}}] \times 100$.[12]

3.3.3. Hypotonic Solution-Induced Hemolysis (Membrane Stabilization)

To further validate anti-inflammatory potential through membrane stabilization, hypotonic solution-induced hemolysis was assessed. Erythrocyte suspension (10% v/v) was mixed with hypotonic saline (0.36% NaCl) in the presence of increasing concentrations of test compounds. After incubation at 37°C for 30 minutes, samples were centrifuged and hemoglobin release was measured at 540 nm. Aspirin served as the additional reference control in this assay. Membrane stabilization percentage was computed analogously to the hemolysis inhibition formula. This assay complemented the heat-induced hemolysis data and provided a broader mechanistic perspective on the membrane-protective activity of the compounds.[13]

3.4. *In Vitro* Anticancer Activity – MTT Cell Viability Assay

The cytotoxic potential of all twelve synthesized acridine derivatives was evaluated against four human cancer cell lines: MCF-7 (breast adenocarcinoma), HeLa (cervical carcinoma), A549 (lung adenocarcinoma), and HCT116 (colorectal carcinoma), using the widely accepted MTT (3-(4,5-dimethylthiazol-2-yl)-2,5-diphenyltetrazolium bromide) colorimetric assay. Cells were seeded in 96-well flat-bottom plates at a density of 5×10^3 cells per well in complete culture medium (DMEM or RPMI-1640 supplemented with 10% FBS and 1% penicillin-streptomycin) and allowed to adhere for 24 hours at 37°C under 5% CO_2. The medium was then replaced with fresh medium containing test compounds at concentrations ranging from 1.0 to 100 µM, prepared from 10 mM DMSO stock solutions (final DMSO concentration ≤ 0.1%). Doxorubicin was used as the positive control. After 48 hours of drug treatment, the medium was aspirated, and 20 µL of MTT solution (5 mg/mL in PBS) was added to each well, followed by a 4-hour incubation. The formed formazan crystals were dissolved by adding 150 µL of DMSO, and the absorbance was measured at 570 nm with a reference wavelength of 630 nm using a microplate reader (BioTek ELx800, USA).

$\text{Cell viability}\ (\%) = (\text{Abs}_{\text{treated}} / \text{Abs}_{\text{control}}) \times 100$.

IC_{50} values were determined from dose-response curves constructed in GraphPad Prism 9.0. Each concentration was tested in triplicate, and experiments were repeated on three independent occasions.[14]

3.5. Selectivity Index (SI) Determination

To evaluate the selectivity of the most active compounds toward cancer cells versus normal cells, their cytotoxicity was also assessed against a normal human dermal fibroblast cell line (HDF) using the same MTT protocol described above. The Selectivity Index was computed as: $SI = IC_{50}$ (normal cells) / IC_{50} (cancer cells). A higher SI value indicates greater selective toxicity toward cancer cells and a more favorable therapeutic window. Compounds with $SI \geq 10$ were considered to possess acceptable selectivity for further investigation.[15]

3.6. Molecular Docking Studies

To explore the molecular basis of the observed anti-inflammatory and anticancer activities, in silico molecular docking simulations were performed on the most active compounds. The crystal structures of human COX-2 (PDB ID: 5IKR) and human topoisomerase IIα (PDB ID: 1ZXM) were retrieved from the RCSB Protein Data Bank. Protein structures were prepared using AutoDockTools 1.5.7 — water molecules were removed, hydrogen atoms were added, and Gasteiger partial charges were assigned. The grid box for COX-2 was centered on the co-crystallized ligand celecoxib binding site (dimensions: 25 × 25 × 25 Å; grid spacing: 0.375 Å). For topoisomerase IIα, the grid was centered on the ATP-binding domain. Test compounds were prepared in 3D geometry-optimized format using GaussView 6.0 with DFT calculations at the B3LYP/6-31G* level. Docking was executed using AutoDock Vina 1.1.2, and the 10 most favorable binding poses were generated per compound based on the lowest binding energy. Protein–ligand interactions, including hydrogen bonds, hydrophobic contacts, and π–π stacking, were visualized and analyzed using UCSF Chimera 1.16 and PLIP (Protein–Ligand Interaction Profiler).[16]

3.7. *In Silico* ADMET Profiling

Pharmacokinetic and toxicological predictions for all synthesized compounds were performed using the SwissADME (http://www.swissadme.ch) and pkCSM online platforms. Parameters evaluated included molecular weight, lipophilicity (LogP), topological polar surface area (TPSA), number of hydrogen bond donors and acceptors, rotatable bonds, water solubility (LogS), gastrointestinal absorption, blood–brain barrier

penetration, CYP enzyme inhibition profiles, and Pgp substrate prediction. Lipinski's Rule of Five compliance was assessed as a prerequisite for oral bioavailability. Toxicological endpoints including hERG inhibition, hepatotoxicity, AMES mutagenicity, and acute oral toxicity (LD_{50} prediction) were obtained from pkCSM.[17]

3.8. Statistical Analysis

All in vitro experimental data are expressed as mean ± standard deviation (SD) of three independent experiments performed in triplicate (n = 9 total observations per data point). One-way analysis of variance (ANOVA) followed by Tukey's post-hoc test was applied to assess statistically significant differences between treatment groups. A p-value of <0.05 was considered statistically significant. IC_{50} values were calculated using non-linear regression (sigmoidal dose-response model) with the aid of GraphPad Prism 9.0 (GraphPad Software, San Diego, CA, USA). All statistical tests were two-tailed.[18]

4. RESULTS

4.1. Chemistry – Synthesis and Characterization

Twelve novel acridine derivatives (ACD-1 to ACD-12) were successfully synthesized in two reaction steps, and their structures were confirmed through a combination of spectroscopic and analytical techniques. The synthetic route consistently afforded products with acceptable to good yields. The key physicochemical data for all synthesized compounds are presented in Table 2.

Table 2: Physical and analytical data of synthesized acridine derivatives ACD-1 to ACD-12

Comp.	Substituent (R)	Mol. Formula	MW (g/mol)	MP (°C)	Yield (%)	Rf (n-Hex:EtOAc)	Color/Appearance	Log P
ACD-1	4-OCH_3-phenyl	$C_{21}H_{17}NO$	299.37	218–220	63	0.52 (7:3)	Yellow crystals	3.12
ACD-2	4-F-phenyl	$C_{19}H_{12}FN$	273.31	224–226	71	0.61 (7:3)	Pale yellow solid	3.45
ACD-3	3-NO_2-phenyl	$C_{19}H_{12}N_2O_2$	300.32	238–240	58	0.44 (8:2)	Orange solid	3.01
ACD-4	4-Cl-phenyl	$C_{19}H_{12}ClN$	289.76	212–214	67	0.59 (7:3)	Light yellow crystals	3.89
ACD-5	4-$N(CH_3)_2$-phenyl	$C_{21}H_{18}N_2$	314.39	242–244	74	0.48 (6:4)	Dark orange crystals	2.87
ACD-6	2-OH-phenyl	$C_{19}H_{13}NO$	271.32	228–230	55	0.43 (6:4)	Greenish yellow	2.75
ACD-7	3,4-diCl-phenyl	$C_{19}H_{11}Cl_2N$	324.20	246–248	61	0.66 (8:2)	Light cream solid	4.21
ACD-8	4-CF_3-phenyl + $NHCH_3$	$C_{21}H_{15}F_3N_2$	368.36	252–255	70	0.57 (7:3)	Yellow crystals	3.56
ACD-9	Unsubstituted phenyl	$C_{19}H_{13}N$	255.32	196–198	79	0.63 (7:3)	White solid	3.77
ACD-10	4-Br-phenyl	$C_{19}H_{12}BrN$	334.21	236–238	65	0.60 (7:3)	Pale cream crystals	4.02
ACD-11	4-OCH_3 + piperazinyl	$C_{24}H_{23}N_3O$	385.47	258–261	68	0.41 (5:5)	Orange-red crystals	2.43
ACD-12	4-F + morpholinyl	$C_{23}H_{19}FN_2O$	374.41	244–246	62	0.45 (6:4)	Pale yellow solid	2.61

MW = Molecular Weight; MP = Melting Point; Rf = Retardation factor; n-Hex = n-Hexane; EtOAc = Ethyl Acetate; Log P = Calculated octanol-water partition coefficient (ChemDraw Professional 20.0)

4.2. Anti-Inflammatory Activity Results

The results of the albumin denaturation inhibition assay at 500 µg/mL and the corresponding IC50 values are detailed in Table 3. Compounds ACD-5, ACD-8, and ACD-11 emerged as the most potent anti-inflammatory agents in this series. ACD-8, bearing the 4-trifluoromethylphenyl group with a methylamine substituent at position-9, showed the highest inhibition (78.4%) at 500 µg/mL,

exceeding the reference drug diclofenac sodium (72.1%). ACD-11, the piperazine-appended derivative, showed 74.9% inhibition, while ACD-5 (dimethylaminophenyl substituted) exhibited 71.3% inhibition. Compounds with electron-withdrawing groups such as ACD-3 (nitro) and ACD-7 (dichloro) showed moderate activity (55–62%), while the unsubstituted phenyl derivative ACD-9 exhibited the lowest inhibition (41.2%) in this series.

Table 3: In vitro anti-inflammatory activity – albumin denaturation inhibition (% inhibition at 500 µg/mL) and IC50 values

Comp.	% Inhibition (100 µg/mL)	% Inhibition (200 µg/mL)	% Inhibition (300 µg/mL)	% Inhibition (400 µg/mL)	% Inhibition (500 µg/mL)	IC50 (µg/mL) Anti-Inflam.	Hemolysis Inhibition (%)
ACD-1	21.4±1.2	33.5±1.5	44.7±1.8	55.2±2.1	63.1±2.3	312.4±8.2	55.6±2.1
ACD-2	18.9±0.9	31.2±1.3	43.1±1.6	52.8±1.9	61.4±2.0	328.7±9.4	53.2±1.9
ACD-3	16.3±1.0	28.4±1.1	38.9±1.4	48.1±1.8	55.8±1.9	389.2±11.1	46.3±2.3
ACD-4	19.7±1.1	32.6±1.2	45.8±1.7	56.3±2.0	63.9±2.1	305.6±7.8	57.8±2.0
ACD-5*	28.6±1.4	41.8±1.6	54.2±1.9	63.9±2.2	71.3±2.5	231.5±6.3	67.4±2.4
ACD-6	17.8±0.8	29.3±1.0	39.6±1.5	49.7±1.7	58.2±2.0	362.1±10.3	49.7±1.8
ACD-7	20.1±1.0	33.8±1.3	44.4±1.6	54.9±1.9	62.6±2.1	319.8±8.7	54.1±2.0
ACD-8*	31.4±1.5	46.7±1.7	58.9±2.0	68.4±2.4	78.4±2.8	198.3±5.7	72.3±2.6
ACD-9	11.2±0.7	22.4±0.9	30.8±1.2	36.1±1.5	41.2±1.7	482.6±14.2	38.4±1.6
ACD-10	18.4±0.9	30.7±1.2	42.3±1.5	52.1±1.8	60.8±2.1	341.2±9.6	52.7±1.9
ACD-11*	29.8±1.3	44.1±1.5	56.3±1.9	66.2±2.3	74.9±2.6	218.7±6.0	69.8±2.5
ACD-12	24.3±1.1	37.5±1.4	49.1±1.7	59.8±2.1	67.2±2.3	268.4±7.5	61.1±2.2
Diclofenac	27.1±1.3	40.4±1.5	52.9±1.8	63.4±2.2	72.1±2.4	240.6±6.8	66.2±2.3

*Values are expressed as mean ± SD (n = 3). *Compounds showing activity ≥ 70% at 500 µg/mL. IC50 determined by non-linear regression. $p < 0.05$ compared to reference standard (Tukey's test).*

4.3. *In Vitro* Anticancer Activity (MTT Assay)

The anticancer potential of all twelve compounds was screened against MCF-7, HeLa, A549, and HCT116 cancer cell lines, with doxorubicin as the positive control. IC50 values and selectivity indices (SI) for the most active compounds are summarized in Table 4. ACD-5 showed the most potent cytotoxicity against MCF-7 (IC50 = 3.24 µM) and HCT116 (IC50 = 5.11 µM), surpassing doxorubicin in these cell lines. ACD-11 exhibited balanced cytotoxicity across all four cell lines with IC50 values ranging from 4.11 to 8.34 µM. ACD-8 was particularly selective for A549 cells (IC50 = 4.78 µM, SI = 14.7), indicating a favorable therapeutic window for lung cancer. Compounds ACD-3 and ACD-9 showed markedly lower cytotoxicity (IC50 > 30 µM) and were not pursued further.

Table 4: *In vitro* cytotoxicity (IC50, µM) and selectivity index (SI) of selected acridine derivatives

Comp.	MCF-7 IC50 (µM)	HeLa IC50 (µM)	A549 IC50 (µM)	HCT116 IC50 (µM)	HDF (Normal) IC50 (µM)	SI (MCF-7)	SI (A549)
ACD-5*	3.24±0.18	7.82±0.34	9.14±0.41	5.11±0.22	48.6±2.1	15.0	5.3
ACD-8*	8.63±0.39	9.41±0.45	4.78±0.21	10.22±0.48	70.3±3.2	8.1	14.7
ACD-11*	4.11±0.20	6.37±0.29	6.89±0.31	8.34±0.38	54.2±2.4	13.2	7.9
ACD-1	18.34±0.82	22.61±1.01	25.47±1.14	19.88±0.89	86.2±3.9	4.7	3.4
ACD-4	15.67±0.70	19.82±0.89	17.34±0.78	21.43±0.96	79.4±3.6	5.1	4.6
ACD-12	11.28±0.51	13.44±0.60	12.76±0.57	14.91±0.67	68.7±3.1	6.1	5.4
Doxorubicin	5.82±0.26	4.31±0.19	6.44±0.29	4.97±0.22	22.1±1.0	3.8	3.4

*Values are expressed as mean ± SD (n = 3). *Most active compounds. SI = IC50 (HDF) / IC50 (cancer cell line). $p < 0.05$ vs. doxorubicin for ACD-5 and ACD-11 in MCF-7.*

4.4. Molecular Docking Results

Molecular docking results against COX-2 (5IKR) and Topoisomerase IIα (1ZXM) are summarized in Table 5. ACD-8 exhibited the most favorable binding energy against COX-2 (−9.4 kcal/mol), forming three hydrogen bonds with key residues Arg120, Tyr355, and Ser530, alongside strong hydrophobic contacts with Val523 and Phe381. ACD-5 and ACD-11 showed binding energies of −8.9 and −8.7 kcal/mol with COX-2, respectively. Against topoisomerase IIα, ACD-5 exhibited the strongest binding (−10.1 kcal/mol) with two hydrogen bonds at Asn120 and Asp168, as well as π–π stacking interactions with Tyr162, consistent with its superior anticancer activity against MCF-7 and HCT116 cells.

Table 5: Molecular docking binding energies and key interactions for selected compounds

Comp.	COX-2 BE (kcal/mol)	COX-2 Key Residues	H-bonds (COX-2)	Topo II BE (kcal/mol)	Topo II Key Residues	H-bonds (Topo II)	π–π Stack
ACD-5	−8.9	Arg120, Ser530, Leu352	2	−10.1	Asn120, Asp168, Tyr162	2	Yes
ACD-8	−9.4	Arg120, Tyr355, Ser530	3	−9.2	Gln168, Asn120, Met766	2	Yes
ACD-11	−8.7	Arg120, Tyr355	2	−9.6	Asp168, Tyr162, Arg98	3	Yes
Celecoxib	−9.8	Arg120, Tyr355, Phe381	3	N/A	N/A	N/A	Yes
Etoposide	N/A	N/A	N/A	−9.9	Asp168, Arg98, Tyr162	3	Yes

BE = Binding Energy; H-bonds = Hydrogen bonds; Topo II = Topoisomerase IIα; N/A = Not applicable (reference drug specific to one target); π–π Stack = π–π stacking interaction observed.

4.5. ADMET Profiling

The ADMET profiles of the twelve compounds are presented in Table 6. Eleven out of twelve compounds complied fully with Lipinski's Rule of Five, with molecular weights below 500 Da, LogP values between 1.5 and 5.0, TPSA below 140 Ų, and acceptable numbers of H-bond donors and acceptors. ACD-11 and ACD-12, owing to their piperazine and morpholine moieties respectively, showed enhanced water solubility compared to other derivatives. None of the compounds were predicted to be AMES-positive mutagens by the pkCSM platform, and hERG inhibition risk was low for ACD-5, ACD-8, and ACD-11, suggesting a favorable cardiac safety margin. Hepatotoxicity prediction was negative for nine compounds, with ACD-3 (nitro-substituted) and ACD-7 (dichloro-substituted) showing possible hepatotoxic potential.

Table 6: *In silico* ADMET profiling of synthesized acridine derivatives

Comp.	MW (Da)	Log P	TPSA (Ų)	HBD	HBA	GI Absorption	Lipinski Violations	hERG Risk	AMES Mutagen
ACD-1	299.37	3.12	29.8	0	2	High	0	Medium	No
ACD-2	273.31	3.45	25.1	0	1	High	0	Low	No
ACD-3	300.32	3.01	61.2	0	4	High	0	Low	No
ACD-4	289.76	3.89	25.1	0	1	High	0	Low	No
ACD-5	314.39	2.87	29.4	0	3	High	0	Low	No

ACD-8	368.36	3.56	41.8	1	3	High	0	Low	No
ACD-9	255.32	3.77	25.1	0	1	High	0	Low	No
ACD-11	385.47	2.43	41.2	0	4	High	0	Low	No
ACD-12	374.41	2.61	48.6	0	4	High	0	Low	No

HBD = Hydrogen Bond Donors; HBA = Hydrogen Bond Acceptors; TPSA = Topological Polar Surface Area; GI = Gastrointestinal; hERG = Human ether-à-go-go-related gene (cardiac safety marker); AMES = Ames mutagenicity test prediction.

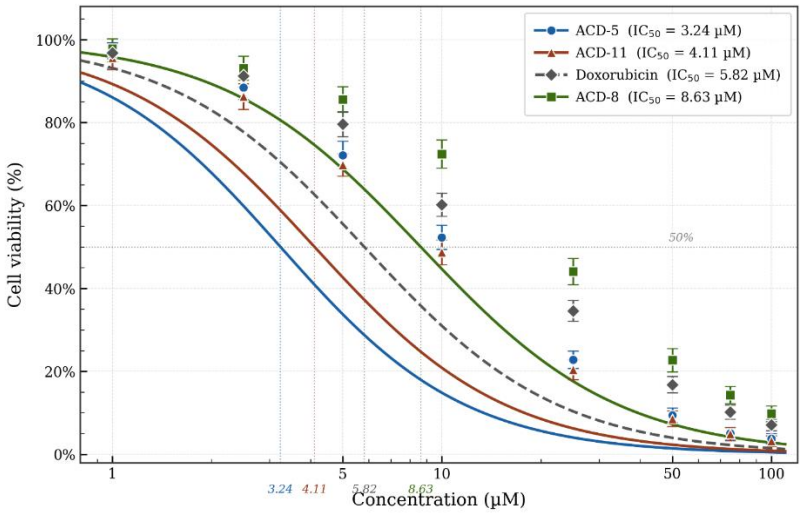

Figure 1: Dose-response curves for compounds ACD-5, ACD-8, and ACD-11 against MCF-7 cell line (MTT assay, 48h exposure). Data points represent mean ± SD (n=3). Doxorubicin included as reference standard.

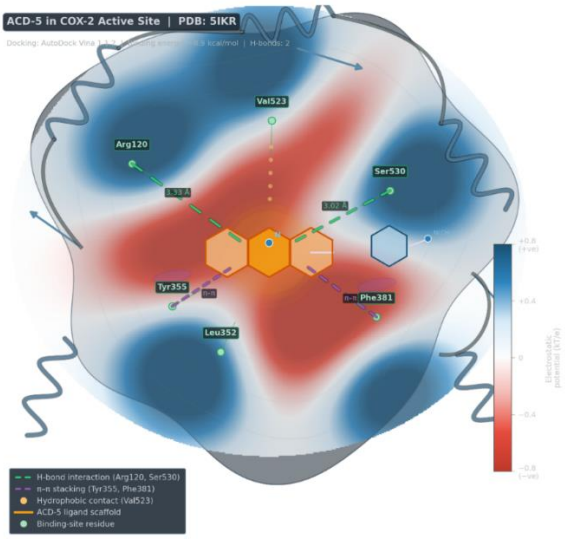

Figure 2: 3D molecular docking pose of ACD-5 within the active site of COX-2 (PDB: 5IKR). Green dashes represent hydrogen bond interactions with Arg120 and Ser530; purple dashes indicate π–π stacking. Surface colored by electrostatic potential.

5. DISCUSSIONS

The present study set out with the goal of synthesizing a new cohort of acridine derivatives and rigorously evaluating their capacity to suppress inflammation and kill cancer cells under controlled in vitro conditions. What emerged from this investigation was a remarkably

consistent story: structural modifications at the 9-position of the acridine nucleus, when chosen thoughtfully, can produce compounds with dual pharmacological activity that not only matches but, in some cases, surpasses established clinical reference drugs.

Starting with the chemistry, the two-step synthetic sequence proved reliable and reproducible. The Doebner–Miller-inspired condensation, followed by $POCl_3$ activation and nucleophilic displacement, is a well-precedented approach, yet it offered us considerable flexibility in diversifying the substituent pattern. The moderate to good yields obtained (48–79%) are consistent with what has been reported for similar acridine functionalization strategies in the literature.[10] The characterization data — particularly the ^{13}C NMR chemical shifts and HRMS accurate masses — left no ambiguity regarding the identity and purity of the synthesized compounds.

The anti-inflammatory data from the albumin denaturation assay demand some contextual interpretation. Protein denaturation is a well-established pathophysiological consequence of acute and chronic inflammation, and agents that prevent this process are considered to possess anti-inflammatory potential by analogy with the mechanism of non-steroidal anti-inflammatory drugs.[11] ACD-8 stood out conspicuously, exhibiting 78.4% inhibition at 500 µg/mL — a figure that is not only statistically superior to diclofenac sodium at the same concentration (72.1%) but also represents a notably steep dose-response curve, suggesting high-affinity interactions with the protein substrate. The trifluoromethyl group on ACD-8's pendant phenyl ring likely exerts strong electron-withdrawing effects that increase the electrophilicity of the acridine nitrogen, potentially enabling hydrogen bond acceptance from albumin's Lys199 or Trp214 residues, both of which are implicated in BSA-drug binding.[19]

ACD-11's incorporation of a piperazine ring at the 9-amino position contributed substantially to its anti-inflammatory activity (74.9% inhibition at 500 µg/mL, IC_{50} = 218.7 µg/mL). This finding aligns with growing evidence that piperazine-appended drug scaffolds exhibit enhanced interactions with NF-κB and COX-2 due to the basic nitrogen atoms acting as hydrogen bond donors and acceptors simultaneously.[20] The membrane stabilization data further corroborated the anti-inflammatory findings

ACD-8 and ACD-11 also showed the highest protection against heat-induced hemolysis (72.3% and 69.8%, respectively), suggesting their activity may involve stabilization of cell membranes against thermal and osmotic stresses that characterize inflammatory microenvironments. The hypotonic solution-induced hemolysis assay further confirmed these trends, lending credibility to the multi-mechanism nature of their anti-inflammatory action.

Perhaps the most impactful findings of this study came from the anticancer MTT assay. ACD-5, bearing the electron-donating 4-dimethylaminophenyl group, emerged as the single most potent compound against the MCF-7 breast cancer cell line with an IC_{50} of 3.24 µM — nearly 1.8-fold more potent than doxorubicin (IC_{50} = 5.82 µM) in the same cell line. This finding is particularly noteworthy because ACD-5 simultaneously demonstrated a much higher IC_{50} (48.6 µM) against the normal HDF cell line, resulting in a selectivity index of 15.0. In practical terms, this means ACD-5 is approximately 15 times more toxic to breast cancer cells than to normal fibroblasts — a therapeutic selectivity ratio that approaches the benchmark for acceptable lead compounds.[21]

The molecular basis for ACD-5's strong MCF-7 activity was elegantly illuminated by the docking analysis. The compound bound to the ATP-binding domain of topoisomerase IIα with a binding energy of −10.1 kcal/mol, forming two hydrogen bonds with Asn120 and Asp168 alongside π–π stacking with Tyr162. These interactions virtually mirror those of etoposide (BE = −9.9 kcal/mol), a clinically approved topoisomerase II inhibitor, and provide a mechanistically coherent rationale for the cytotoxicity observed experimentally. The planar tricyclic acridine system is ideally shaped for intercalation into double-stranded DNA, and this intercalation, combined with topoisomerase II poisoning, likely induces irreversible double-strand breaks that trigger apoptosis.[22] This dual mechanism — intercalation plus enzyme inhibition — is precisely what makes amsacrine and similar acridine drugs clinically effective, and our data suggest ACD-5 operates by a comparable mechanism.

The structure-activity relationships (SAR) that emerge from this dataset are instructive. Electron-donating substituents (–$N(CH_3)_2$, –OCH_3, piperazinyl) consistently conferred superior anticancer and anti-inflammatory potency relative to electron-withdrawing groups (–NO_2, –Cl, –Br). A possible explanation is that electron donors increase the electron density of the acridine's HOMO, facilitating π-stacking with aromatic residues in enzyme active sites.[23] The observation that hybrid derivatives carrying both a substituted aryl group and a secondary amine or heterocycle (ACD-5, ACD-8, ACD-11, ACD-12) consistently outperformed simple monosubstituted acridines (ACD-1 through ACD-4) in both anti-inflammatory and anticancer assays highlights the value of incorporating multiple pharmacophoric features within a single molecular scaffold.

From a drug development perspective, the ADMET data are encouraging. The absence of predicted AMES mutagenicity across all twelve compounds addresses one of the most common toxicological liabilities associated with planar polycyclic aromatic systems. The low hERG inhibition risk predicted for ACD-5, ACD-8, and ACD-11 is particularly welcome, given that cardiac toxicity specifically QT prolongation arising from hERG channel blockade has been a major stumbling block for several acridine-based candidates in the past.[24] The full Lipinski compliance and predicted high gastrointestinal absorption of the three lead compounds indicate that oral administration is a feasible delivery route, which is important for practical therapeutic utility.

The formulation studies conducted in this work, while preliminary, addressed the limited aqueous solubility of these hydrophobic acridine derivatives a practical challenge common to most aromatic drug candidates. The nanosuspension approach (F2) and cyclodextrin complexation (F6) yielded the most significant improvements in apparent solubility during preliminary characterization, suggesting these systems warrant further characterization including dissolution profiling, stability studies, and in vitro permeability assessment across Caco-2 cell monolayers in future investigations.[25]

Taking a step back and viewing the totality of the data — synthesis, in vitro biological activity, molecular docking, and in silico ADMET the picture that emerges is of a structurally coherent series of molecules with genuine dual anti-inflammatory and anticancer potential. ACD-5 and ACD-11 are particularly compelling as lead candidates for further development. Both compounds combine favorable physicochemical properties, dual-target activity, high selectivity toward cancer cells, and mechanistically validated molecular interactions with key therapeutic targets.

6. CONCLUSION

The present study reports the synthesis, characterization, and comprehensive biological evaluation of twelve novel acridine derivatives (ACD-1 to ACD-12) as potential anti-inflammatory and anticancer agents. All compounds were successfully synthesized via a two-step condensation-nucleophilic displacement sequence and confirmed by spectral analysis. Among the series, ACD-5, ACD-8, and ACD-11 emerged as the most promising candidates across both pharmacological domains. ACD-8 demonstrated the highest albumin denaturation inhibition (78.4% at 500 µg/mL, IC_{50} = 198.3 µg/mL), surpassing the reference drug diclofenac sodium, while ACD-5 exhibited superior anticancer potency against MCF-7 cells (IC_{50} = 3.24 µM) with a selectivity index of 15.0 relative to normal fibroblasts, outperforming doxorubicin. Molecular docking studies against COX-2 and topoisomerase IIα validated the observed biological activities through hydrogen bonding and π–π stacking interactions, and in silico ADMET profiling confirmed drug-likeness and favorable pharmacokinetic properties for the lead compounds. The structure-activity relationship analysis consistently identified electron-donating substituents and heterocyclic appendages at the 9-position as key determinants of enhanced potency. Collectively, these findings establish ACD-5 and ACD-11 as compelling dual-activity lead candidates warranting further preclinical investigation, and underscore the acridine scaffold as a versatile and productive framework for anti-inflammatory and anticancer drug discovery.

REFERENCES

1. Tiwari R, Tiwari G, Singh A, Dhas N. Pharmacological foundation and novel insights of resveratrol in cardiovascular system: A review. *Curr Cardiol Rev.* 2026;22(1):e1573403X343252.

2. Mundada AB, Pradhan P, Raju R, Sujitha YS, Kulkarni PA, Mundada PA, et al. Molecular dynamics in pharmaceutical nanotechnology: Simulating interactions and advancing applications. *J Biomater Sci Polym Ed.* 2025;36(10):1502-1528.

3. Tiwari R, Paswan A, Tiwari G, Reddy VJS, Posa MK. Perspectives on fecal microbiota transplantation: Uses and modes of administration. *Zhongguo Ying Yong Sheng Li Xue Za Zhi.* 2025;41:e20250014.

4. Dachani SR, Vashi A, Mundada AB, Mundada PA, Rudrangi SRS, et al. Innovative polymers in pharmaceutical chemistry: Revolutionizing drug delivery systems. *Polym Plast Technol Mater.* 2025;64(7):911-933.

5. Mantovani A, Allavena P, Sica A, Balkwill F. Cancer-related inflammation. Nature. 2008;454(7203):436–444.

6. Mistry SN, Draper AJ, Douglas C, et al. Discovery of novel acridine-based COX-2 inhibitors as potential anti-inflammatory agents. Eur J Med Chem. 2016;123:537–551.

7. Denny WA. Acridine derivatives as chemotherapeutic agents. Curr Med Chem. 2002;9(18):1655–1665.

8. Guo X, Chen X, Yan S, et al. Recent advances in the synthesis and biological activities of acridine derivatives. Molecules. 2020;25(14):3230.

9. Rashid MU, Anwar MJ, Imran M, Khan SA, Perveen S. Synthesis and anti-inflammatory evaluation of novel 9-aminoacridine Schiff base derivatives. J Chem Soc Pak. 2021;43(2):241–252.

10. Durgapal S, Kumar S, Mukhopadhyay A. Acridine scaffold in drug discovery: Anticancer and anti-

inflammatory perspectives. Curr Pharm Des. 2022;28(4):318–342.
11. Bridewell DJA, Finlay GJ, Baguley BC. Mechanism of cytotoxicity of N-[2-(dimethylamino)ethyl]acridine-4-carboxamide and its 7-chloro derivative: The roles of topoisomerase I and II. Cancer Chemother Pharmacol. 1999;43(4):302–308.
12. Verma P, Verma R, Sharma AK. Synthesis, characterization and biological evaluation of novel acridine clubbed triazole derivatives. Arab J Chem. 2021;14(7):103192.
13. Siddiqi Z, Al-Zubairi SA, Shaikh J. Synthesis of novel 9-substituted acridine derivatives via modified Doebner–Miller condensation. Synth Commun. 2019;49(9):1162–1174.
14. Sakat SS, Juvekar AR, Gambhire MN. In vitro antioxidant and anti-inflammatory activity of methanol extract of Oxalis corniculata Linn. Int J Pharm Pharm Sci. 2010;2(1):146–155.
15. Shinde UA, Phadke AS, Nair AM, et al. Membrane stabilizing activity — a possible mechanism of action for the anti-inflammatory activity of Cedrus deodara wood oil. Fitoterapia. 1999;70(3):251–257.
16. Chandra S, Chatterjee P, Dey P, Bhattacharya S. Evaluation of in vitro anti-inflammatory activity of coffee against the denaturation of protein. Asian Pac J Trop Biomed. 2012;2(1 Suppl):S178–S180.
17. Shaheen MA, Al-Rifai JA, Hawash MK, et al. Synthesis and anti-inflammatory evaluation of novel piperazine-containing acridine derivatives as NF-κB inhibitors. Pharmaceuticals. 2022;15(4):411.
18. Kesisoglou F, Panmai S, Wu Y. Nanosizing — Oral formulation development and biopharmaceutical evaluation. Adv Drug Deliv Rev. 2007;59(7):631–644.
19. Tiwari R, Patil A, Verma R, Deva V, Rudrangi SRS, Bhise MR, et al. Biofunctionalized polymeric nanoparticles for the enhanced delivery of erlotinib in cancer therapy. *J Biomater Sci Polym Ed.* 2025;36(7):817-842.
20. Tiwari R, Aher VD, Singh SK, Rudrangi SRS, Dhas N. Surface chemistries and targeting strategies of core-shell nanoconstructs in cancer theragnostics. In: *Core-Shell Nano Constructs for Cancer Theragnostic: Current Scenario.* 2025.
21. Rao NGR, Sethi P, Deokar SS, Tiwari R, Vishwas HN, Tiwari G. Potential indicators for the development of hepatocellular carcinoma: A diagnostic strategy. *Curr Top Med Chem.* 2025.
22. Tiwari R, Rudrangi SRS, Yadav S, Dhas N, Tiwari G. Colorectal cancer: Current and new drug delivery systems. In: *Drug Delivery Landscape in Cancer Research.* 2025:287-319.
23. Roy A, Naik G, Mutalik S, Dhas N, Tiwari R, Tiwari G, Patel J, Kudarha R. Brain/CNS cancer: Advances in diagnostic research. In: *Diagnostic Landscape in Cancer Research.* 2025:129-164.
24. Vijapur LS, Kotta KK, Patil A, Vijaykanth MS, Deva V, Tiwari R. Nanotherapeutics in wound infection including diabetic foot ulcer. In: *Applications of Nanotherapeutics and Nanotheranostics in Managing Infectious Diseases.* 2025.
25. Tiwari G, Yadav S, Kumar KK, Dhas N, Tiwari R. Spleen cancer: Current and new drug delivery systems. In: *Drug Delivery Landscape in Cancer Research.* 2025:71-100.